Flexible Solid-State Supercapacitors Based on Three-Dimensional Graphene Hydrogel Films

Yuxi Xu,[†] Zhaoyang Lin,[†] Xiaoqing Huang,[‡] Yuan Liu,[‡] Yu Huang,[‡,§] and Xiangfeng Duan[†,§,*]

[†]Department of Chemistry and Biochemistry, University of California, Los Angeles, California 90095, United States, [‡]Department of Materials Science and Engineering, University of California, Los Angeles, California 90095, United States, and [§]California Nanosystems Institute, University of California, Los Angeles, California 90095, United States

ABSTRACT Flexible solid-state supercapacitors are of considerable interest as mobile power supply for future flexible electronics. Graphene or carbon nanotubes based thin films have been used to fabricate flexible solid-state supercapacitors with high gravimetric specific capacitances (80−200 F/g), but usually with a rather low overall or areal specific capacitance (3−50 mF/cm^2) due to the ultrasmall electrode thickness (typically a few micrometers) and ultralow mass loading, which is not desirable for practical applications. Here we report the exploration of a three-dimensional (3D) graphene hydrogel for the fabrication of high-performance solid-state flexible supercapacitors. With a highly interconnected 3D network structure, graphene hydrogel exhibits exceptional electrical conductivity and mechanical robustness to make it an excellent material for flexible energy storage devices. Our studies demonstrate that flexible supercapacitors with a 120 μm thick graphene hydrogel thin film can exhibit excellent capacitive characteristics, including a high gravimetric specific capacitance of 186 F/g (up to 196 F/g for a 42 μm thick electrode), an unprecedented areal specific capacitance of 372 mF/cm^2 (up to 402 mF/cm^2 for a 185 μm thick electrode), low leakage current (10.6 μA), excellent cycling stability, and extraordinary mechanical flexibility. This study demonstrates the exciting potential of 3D graphene macrostructures for high-performance flexible energy storage devices.

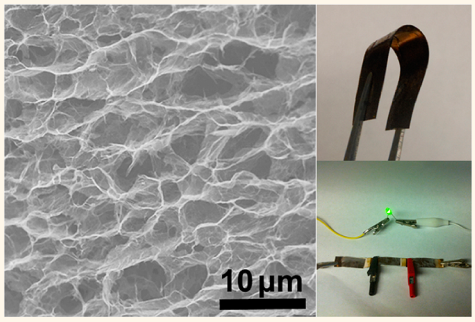

KEYWORDS: energy storage · supercapacitor · graphene · solid-state devices · 3D network · flexible electronics

With portable and flexible electronics becoming increasingly pervasive in our daily lives, there is a growing demand for lightweight, flexible, and highly efficient energy storage devices.[1−4] Supercapacitors are widely recognized as an important class of energy storage devices, because they can provide a high power density, long cycle life, along with the potential to achieve a relatively high energy density close to traditional batteries.[5−7] Considerable efforts have been dedicated to developing high-performance flexible solid-state supercapacitors based on various carbon nanomaterials and their composites.[8−17] As a unique carbon nanomaterial, graphene has attracted intense interest for its promising applications in supercapacitor electrodes,[18−20] mainly due to its excellent conductivity, mechanical flexibility, exceptionally large specific surface area, and chemical stability. Several studies have recently demonstrated the fabrication of flexible solid-state supercapacitors through the assembly of Nafion or ionic liquid functionalized graphene thin films (or reduced graphene oxide films) obtained by a vacuum filtration method.[14−16]

Although graphene can fundamentally provide a specific capacitance value up to 550 F/g,[18] the specific capacitances achieved in most solid-state devices demonstrated to date are typically in the range 80−118 F/g at the current density of 1 A/g, which is largely limited by the parallel restacking of graphene sheets to greatly reduce its active surface area. A unique laser reduction approach was recently used to produce a porous reduced graphene oxide thin film electrode for solid-state supercapacitors with the highest specific capacitance of ~204 F/g.[13] Despite this significant progress, most of the studies on solid-state supercapacitors to date use ultrathin film electrodes (typically around 10 μm thick or less) with a rather low mass loading, and therefore usually with a very low overall or

* Address correspondence to xduan@chem.ucla.edu.

Received for review January 7, 2013 and accepted April 3, 2013.

Published online April 04, 2013
10.1021/nn4000836

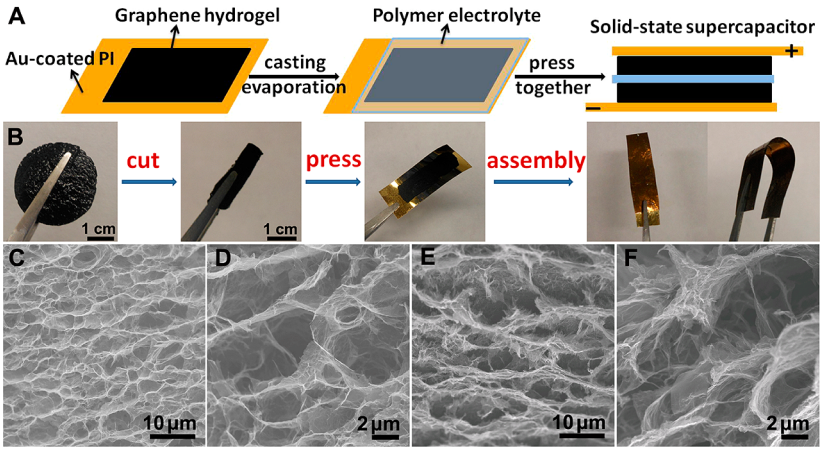

Figure 1. (A) Schematic diagram and (B) photographs of the fabrication process of flexible solid-state supercapacitors based on graphene hydrogel films. (C) Low- and (D) high-magnification SEM images of the interior microstructure of the graphene hydrogel before pressing. (E) Low- and (F) high-magnification SEM images of the interior microstructure of the graphene hydrogel film after pressing.

areal specific capacitance (3−50 mF/cm^2 or less),[13−16] which is not desirable for practical applications. It has also been recognized that supercapacitor electrodes with ultrathin films usually have a smaller internal resistance and better ion diffusion characteristics to result in higher apparent specific capacitance and higher rate capability, which is, however, not always translatable into devices with thicker films and larger mass loading.[9,19]

Recently, graphene-based macroscopic materials with a three-dimensional (3D) porous network have received increasing attention for electrochemical energy storage.[21,22] Typical 3D graphene macrostructures such as graphene hydrogels or aerogels could be easily prepared by one-step chemical reduction of a graphene oxide dispersion, in which flexible graphene sheets partially overlap in 3D space to form interconnected porous microstructure.[23−29] This unique hierarchical architecture not only prevents serious restacking of graphene sheets but also allows electrolytes to freely diffuse inside and through the network. With an exceptionally high surface area (up to 1000 m^2/g based on methylene blue molecular adsorption), these mechanically strong and electrically conductive 3D graphene materials have been directly used as binder-free supercapacitor electrodes with excellent specific capacitances (160−240 F/g), rate capability, and cycling stability.[23−29] However, the superior capacitive performances of these 3D graphene macrostructures were obtained in conventional supercapacitor systems with liquid electrolytes, which requires a relatively complicated encapsulation process to prevent the leakage of liquid electrolytes and is usually not compatible with flexible electronic applications.

Here we report the fabrication of a novel flexible solid-state supercapacitor based on graphene hydrogel films using H_2SO_4-polyvinyl alcohol (PVA) gel as the electrolyte. The integrated device exhibited a high gravimetric specific capacitance (186 F/g at 1 A/g), excellent rate capability (70% retention at 20 A/g), a small leakage current of as little as 10.6 μA, and more importantly an unprecedented area-specific capacitance of 372 mF/cm^2. Furthermore, the device showed little capacitance change while tested under its normal and highly bent conditions and excellent cycling stability with only 8.4% capacitance decay over 10 000 charge/discharge cycles at a current density of 10 A/g, which can be attributed to the exceptional mechanical and electrical robustness of the highly interconnected network structure of graphene hydrogel films. We have further demonstrated the practical use of the solid-state device to light up LEDs, highlighting the significant potential of 3D graphene macrostructures for high-performance flexible energy storage devices.

RESULTS AND DISCCUSION

Figure 1A,B show the processing steps to fabricate graphene hydrogel based solid-state flexible supercapacitors. First, a free-standing graphene hydrogel with a thickness of ∼3 mm was synthesized by a modified hydrothermal reduction method[23,24] and immersed in 1 M H_2SO_4 aqueous solution overnight. The graphene hydrogel was then cut into rectangular strips with a dried weight of ∼3.5 mg and pressed on the gold-coated polyimide substrate under a pressure of ∼1 MPa to form a thin film with an areal mass of ∼2 mg/cm^2. To assemble the solid-state supercapacitor device, a H_2SO_4−PVA aqueous solution (∼10 wt % for both H_2SO_4 and PVA) was slowly poured onto two separate graphene hydrogel films and air-dried at room temperature for 12 h to evaporate excess water. The two graphene hydrogel electrodes were then pressed together under a pressure of ∼1 MPa for 30 min, allowing the polymer gel electrolyte on each electrode to combine into one thin separating layer. The resulting device was highly flexible and robust.

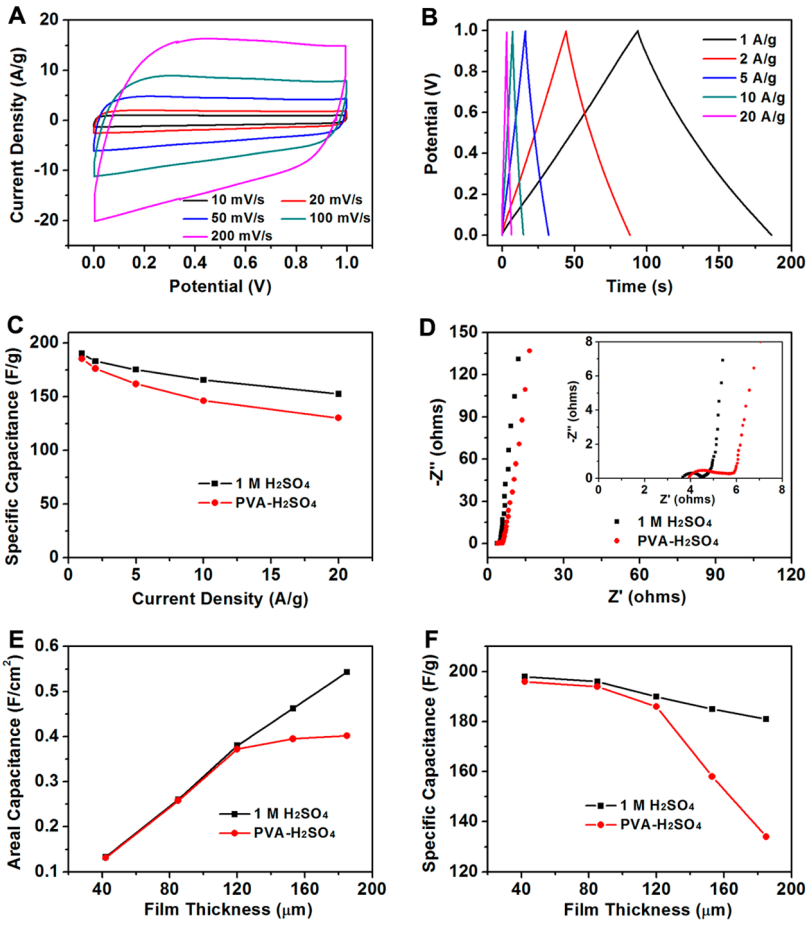

Figure 2. (A) CV and (B) galvanostatic charge/discharge curves of the flexible solid-state device. (C) Comparison of specific capacitances and (D) Nyquist plots of a graphene hydrogel film electrode in H_2SO_4–PVA gel electrolyte and 1 M H_2SO_4 aqueous electrolyte. The inset in (D) shows the magnified high-frequency regions of the Nyquist curves. Thickness dependence of (E) areal capacitance and (F) mass-specific capacitance of a graphene hydrogel film comparing a liquid (1 M H_2SO_4) and a gel (H_2SO_4–PVA) electrolyte at a current density of 1 A/g.

The morphologies of the graphene hydrogel before and after pressing were characterized by scanning electron microscopy (SEM). The as-prepared graphene hydrogels are formed by partial overlapping of graphene sheets *via* hydrophobic and $\pi-\pi$ interactions in 3D space and possess an interconnected porous network with most of its pores having a size of several micrometers (Figure 1C,D). Although the hydrophobic and $\pi-\pi$ interactions are weak interactions, the extended π-conjugation in graphene sheets can allow extended π-stacking interactions between graphene sheets to form strong bindings, resulting in highly robust cross-links in the graphene hydrogels.[23] Upon physical pressing, the 3D graphene framework is substantially compressed from a thickness of ~3 mm to ~120 μm. Moreover, the 3D continuous porous network was well maintained (Figure 1E,F). The porous structure of the graphene hydrogel film was confirmed by nitrogen adsorption and desorption measurements (Figure S1 in the Supporting Information). A typical type-IV isotherm characteristic with a distinct adsorption hysteresis loop indicates there are a lot of relatively large macropores and mesopores in the 3D framework of the graphene hydrogel film (Figure S1A). Brunauer–Emmett–Teller (BET) and Barrett–Joyner–Halenda (BJH) analyses also reveal that the graphene hydrogel film has a high specific surface area of ~414 m^2/g and much of its pore volume (~0.73 cm^3/g) lies in the range 2–70 nm (Figure S1B). Compared with previous compact graphene films obtained by vacuum filtration,[14−16] our graphene hydrogel film provides a favorable porous structure for electrolyte infiltration to make full use of the large electrical double-layer capacitance of graphene hydrogels.

The conductivities of the graphene hydrogel before and after physical pressing were measured to be 7.8 and 192 S/m, respectively, indicating a good electrical connectivity between graphene sheets in graphene hydrogels before and after compressing. We have also tested the mechanical flexibility of graphene hydrogel films (Figure S2 in the Supporting Information). Although the as-prepared graphene hydrogel is easy to beak under bending state (the maximum bending angle is about 30°–40°), the flexibility of the graphene

hydrogel film was greatly enhanced upon physical pressing due to the extrusion of large amounts of entrapped water from the graphene hydrogel and increased contact between the graphene skeleton (Figure S2A in the Supporting Information). The current−voltage curves of the graphene hydrogel film were nearly unchanged at different bending states and remained almost constant after 50 and 100 cycles of bending, revealing the conductance was hardly affected by bending stress (Figure S2B,C in the Supporting Information). The cross-section SEM images of the graphene hydrogel films before and after the bending operation indicate that the interior microstructures of the graphene hydrogel films are well maintained after the bending test and the connectivity between the graphene sheets in the graphene hydrogel films is strong enough for flexible devices (Figure S3 in the Supporting Information).

The capacitive performance of the flexible solid-state supercapacitors was evaluated by cyclic voltammetry (CV) and galvanostatic charge/discharge tests. Figure 2A shows CV curves of the device in the range 0 to 1.0 V at various scan rates. In general, the shape of the CV loop of an ideal electrical double-layer supercapacitor should be rectangular. A large contact resistance could distort the loop to result in an oblique angle.[30] The CV curves of our device are close to rectangular even at a high scan rate of 200 mV/s, indicating an excellent capacitive behavior and low contact resistance. The specific capacitances of the graphene hydrogel film electrode estimated from the CV curves were ∼187 and ∼137 F/g at scan rates of 10 and 200 mV/s, respectively. Consistently, the linear profile of galvanostatic charge and discharge curves and their symmetric triangular shape indicate nearly ideal capacitive characteristics (Figure 2B).

The graphene hydrogel film in the solid-state device exhibited a high specific capacitance of ∼186 F/g at a current density of 1 A/g (Figure 2C), which is very close to the device measured in 1 M H_2SO_4 aqueous electrolyte (∼190 F/g, Figure S4 in the Supporting Information), indicating an efficient infiltration of polymer gel electrolyte into the 3D graphene network. When the current density is increased from 1 to 20 A/g, the solid-state device showed a lower specific capacitance and rate capability (∼130 F/g, 70% retention) than the one in 1 M H_2SO_4 solution (∼152 F/g, 80% retention) (Figure 2C). This could be attributed to higher internal resistance and slower electrolyte diffusion in solid-state devices. This is also confirmed by the Nyquist plots obtained from electrochemical impedance spectroscopy measurements (Figure 2D). Nevertheless, the specific capacitances of the graphene hydrogel film based solid-state supercapacitor are substantially higher than those of most of the previously reported solid-state devices made of carbon nanotubes (50−115 F/g at 1 A/g)[9−12] and graphene films (80−118 F/g at 1 A/g)[14−16] and are comparable to the recently reported laser-reduced graphene oxide thin film supercapacitor (∼204 F/g).[13]

Furthermore, it is important to note that with the 3D graphene hydrogel we can prepare a thin film electrode (∼120 μm) much thicker than that of the previous solid-state devices (∼10 μm or less) and, therefore, achieve an area-specific capacitance (372 mF/cm^2) that is more than 1 order of magnitude larger than previous studies (3−46 mF/cm^2) (Table S1 in the Supporting Information). It has been recognized that supercapacitor electrodes with ultrathin films usually have a smaller internal resistance and better ion diffusion characteristics to result in a higher apparent specific capacitance when normalized by weight, which, however, cannot always be translated into devices with thicker films and larger mass loading.[9,19] The ability to achieve a high specific capacitance of 186 F/g in our thick thin film electrodes further confirms the excellent conducting network of the graphene hydrogel film with a large specific surface area and the excellent infiltration of the electrolyte into the network. Achieving a high areal capacitance while maintaining the flexible quality of the supercapacitors is essential to power portable electronic devices and smart garments (such as mobile phones, notebook computers, and digital cameras),[31] because there is usually a limited amount of surface area to integrate electronics and capacitive materials in these electronic products.[31]

Although it is not surprising that the area-specific capacitance normally scales linearly with the electrode thickness, it is also well known that the area-specific capacitance of solid-state supercapacitors can eventually saturate with the thicker electrode due to the limited infiltration of polymer gel electrolyte into the electrode materials.[9] To this end, we have also investigated the capacitive performances of graphene hydrogel films as a function of electrode thicknesses (∼42−185 μm) in the liquid (1 M H_2SO_4) and gel (H_2SO_4−PVA) electrolytes. Our studies show that the area-specific capacitance exhibits a nearly linear behavior *vs* electrode thickness in liquid electrolyte (1 M H_2SO_4), but starts to saturate in gel electrolytes (H_2SO_4−PVA) when the electrode thickness exceeds 120 μm, with a maximum areal capacitance of 402 mF/cm^2 achieved in a ∼185 μm thick film (Figure 2E). On the other hand, the mass-specific capacitance decreases moderately with the film thickness in liquid electrolyte, and similar behavior is shown in gel electrolyte before the saturation thickness (∼120 μm), beyond which the mass-specific capacitance in the gel electrolyte device degrades rather quickly due to the limited infiltration of the gel electrolyte (Figure 2F). The saturation thickness (120−180 μm) and maximum areal capacitance (402 mF/cm^2) of our devices are much larger than those of previous carbon nanotube thin film supercapacitors (5−10 μm and 30 mF/cm^2,

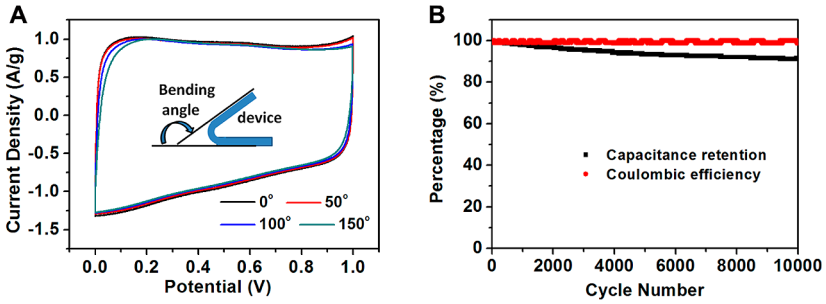

Figure 3. (A) CV curves of the flexible solid-state device at 10 mV/s for different bending angles. (B) Cycling stability of the device at a current density of 10 A/g.

respectively),[9] which has directly enabled us to achieve much larger overall or area-specific capacitance in our devices. These studies further highlight that the use of the 3D graphene hydrogel macrostructures not only provides a highly conductive network for electrical transport but also provides an open network for efficient electrolyte diffusion to enable superior capacitive performance.

Our flexible solid-state supercapacitors also exhibit excellent mechanical robustness in the bending test. The CV curves obtained at various bending angles show nearly the same capacitive behavior (Figure 3A), demonstrating that the change of electrochemical property is negligible under different bending angles. To further characterize the cyclability and performance durability of the solid-state device, galvanostatic charge/discharge tests were carried out up to 10 000 cycles at a high current density of 10 A/g under a 150° bending angle. Remarkably, only 8.4% decay in specific capacitance was observed after 10 000 charge/discharge cycles, and the calculated Coulombic efficiency was always kept in the range 98.8−100% throughout the testing cycles (Figure 3B). Such excellent flexibility and capacitive performance of our device can be attributed to the exceptional mechanical and electrical robustness of the highly interconnected 3D network structure of graphene hydrogel films and the favorable interfacial electrochemical behaviors of the graphene hydrogel film in the H_2SO_4−PVA gel electrolyte.

For practical application, it is important to evaluate the leakage current and self-discharge characteristics of the solid-state devices, which is often not discussed enough in recent studies. In general, our device was first charged to 1.0 V at 2 mA, and then the potential was kept at 1.0 V for 2 h and the current flowing through the supercapacitor was recorded. In this constant-voltage mode, the current through the stabilized device compensates the current loss by the capacitor itself, which can be viewed as the leakage current. For our graphene hydrogel film based solid-state supercapacitor, the current quickly stabilizes at 10.6 μA, which is essentially the leakage current through the device (Figure 4A). This value (1.5 μA per mg electrode) is lower than that of a carbon nanotube/polyaniline composite supercapacitor (17.2 μA, 5.5 μA per mg electrode),[8] indicating a relatively small leakage current and high stability of our supercapacitor devices.[30] The stability of the device and its capability for retaining charges were further demonstrated by a self-discharge test represented by the time course of the open-circuit voltage. As shown in Figure 4B, the device after being charged at 1.0 V for 15 min underwent a rapid self-discharge process in the first half hour, which gradually slowed after several hours. Finally the output voltage of the device reached about 0.4 V after 24 h, which is comparable to previous results of solid-state supercapacitors (0.2−0.5 V).[8,17] These studies demonstrate that our devices exhibit excellent low self-discharge characteristics, which is highly desirable for practical applications in mobile electronics.

We have further tested the lifetime stability of the devices. The electrochemical performances of the device were evaluated 1 week and 1 month after the device was fabricated. The CV and galvanostatic charge/discharge curves show that the capacitive behavior was well retained after 1 week and even 1 month (Figure 4C and D). The specific capacitance of the device showed a rather small decay of 2.5% after the initial week, and the value decayed only 6.2% after 1 month. Further water evaporation could cause a less effective ion diffusion to result in a slow decay in the specific capacitance. It is important to note that this decay saturates over time and eventually stabilizes at a nearly constant value.

To further evaluate the performance of the solid-state devices, we have plotted the Ragone plot to compare our devices with a few typical examples reported in the literature to date (Figure 5). The plot clearly shows that our solid-state supercapacitors exhibit significantly higher energy and power densities compared to most of the previously reported solid-state devices made of carbon nanotube and graphene thin films. Such high energy or power density is achieved in our devices with much thicker film electrodes (~120 μm) and larger mass loading (~2 mg/cm^2) than previous devices. This is particularly significant for practical application of thin film energy storage devices because it can offer orders of magnitude higher

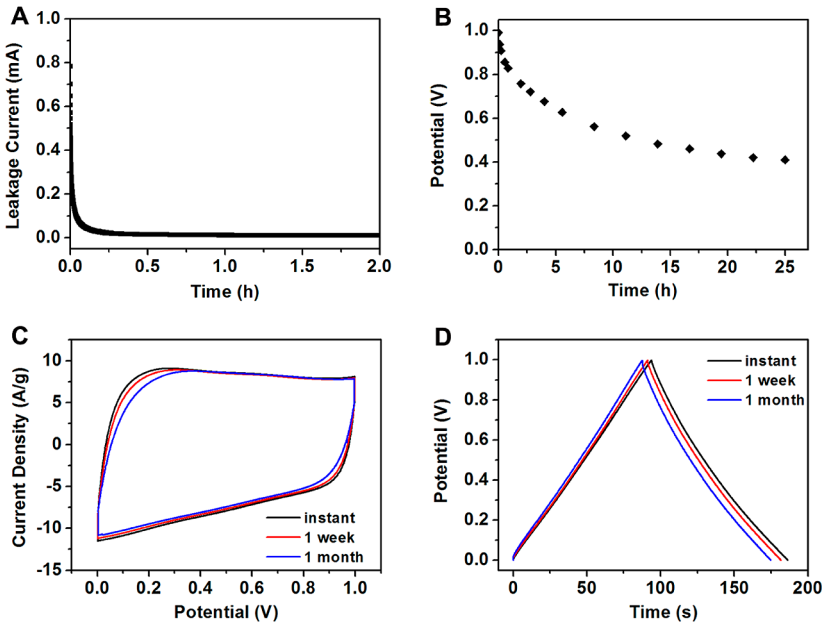

Figure 4. (A) Leakage current curves of the solid-state device charged at 2 mA to 1.0 V and kept at 1.0 V for 2 h. (B) Self-discharge curve of the device after charging at 1.0 V for 15 min. (C) CV curves at 100 mV/s and (D) galvanostatic charge/discharge curves at 1 A/g of a supercapacitor taken at different time durations.

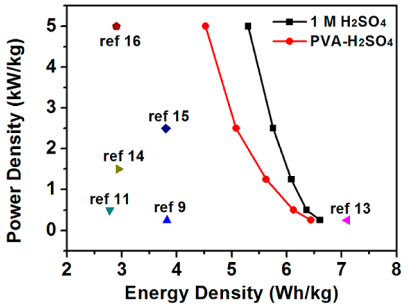

Figure 5. Ragone plots (power density *vs* energy density) comparing the graphene hydrogel film based supercapacitors to previously reported solid-state devices made of carbon nanotubes and graphene thin films.

overall or area-specific capacitance. It should be noted that the power density and energy density shown in Figure 5 are based on the mass of active electrode materials, similar to previous studies for comparison purposes.[9−15] Normalized by the total mass of the entire device (~52 mg), our device exhibits a power density (0.67 kW/kg) and energy density (0.61 Wh/kg) that compare favorably with a solid-state supercapacitor based on papers coated with carbon nanotubes (0.46 kW/kg and 0.12 Wh/kg),[11] but are inferior to the solid-state supercapacitor based on free-standing graphene thin films with no substrates (1.81 kW/kg and 2.9 Wh/kg).[16] We believe the performance based on the total mass of cells can be greatly improved by reducing the thickness of the electrolyte and the substrate as recently demonstrated.[8,32]

The volumetric capacitance of our graphene hydrogel films was calculated to be 31 F/cm^3, which is higher than the values reported for solid-state graphene (9.6 F/cm^3)[13] and polypyrrole (28 F/cm^3)[33] supercapacitors, indicating that graphene hydrogel films could simultaneously achieve large areal capacitance and reasonable volumetric capacitance. It should be noted that nitrogen and boron co-doped graphene aerogels have recently been explored for solid-state supercapacitors,[29] but with a lower specific capacitance (118 F/g at 10 mV/s) and rate capability (45% retention at 100 mV/s) than our graphene hydrogel films, which can be largely attributed to the fact that the aerogels prepared by freeze-drying of the corresponding hydrogels usually have a lower specific surface area and worse electrolyte wettability and diffusion than hydrogels due to the hydrophobic nature of graphene sheets and fusing of many mesopores within the aerogels impelled by gradual growth of ice crystals during the freeze-drying process.[28,34]

To demonstrate the potential usefulness of the graphene hydrogel films based flexible solid-state supercapacitors, we have connected three supercapacitor units in series to make a tandem device. Each supercapacitor unit used here has the same mass loading of graphene hydrogel film (~3.5 mg for one electrode). The tandem device was evaluated by CV and galvanostatic charge/discharge measurements (Figure S5 in the Supporting Information). As shown in Figure 6A and B, the potential window is extended from 1.0 V for a single device to 3.0 V for a tandem device. Meanwhile, the product current (represented by the area under the CV curves) and the charge/discharge time at the same current density are essentially unchanged for the tandem device *vs* individual devices, indicating the capacitive performance of each

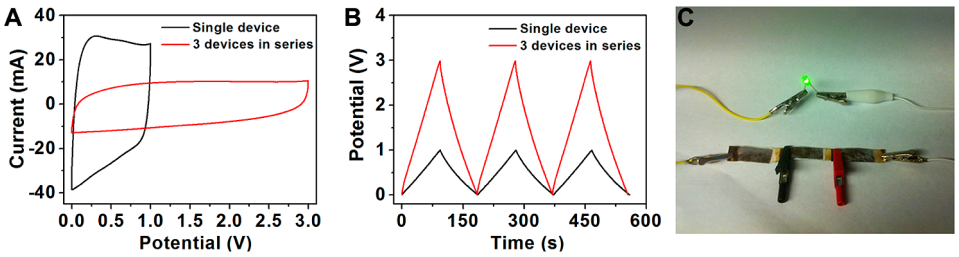

Figure 6. (A) CV curves at 100 mV/s and (B) galvanostatic charge/discharge curves at 3.5 mA of a single solid-state supercapacitor (black) and three supercapacitors in series (red). (C) Photograph of a green LED powered by the three supercapacitors in series.

supercapacitor unit is well retained in the tandem device. Lastly, we have used the tandem device to light up a green light-emitting-diode (LED, the lowest working potential is about 2.0 V) (Figure 6C), demonstrating the practical potential of the flexible supercapacitors.

CONCLUSIONS

We have reported a novel flexible solid-state supercapacitor with 120 μm thick graphene hydrogel films to achieve a high gravimetric specific capacitance (186 F/g at 1 A/g), an unprecedented area-specific capacitance (372 mF/cm^2), excellent rate capability (70% retention at 20 A/g), cycling stability (8.4% capacitance decay over 10 000 charge/discharge cycles), and outstanding mechanical flexibility. The performance of these devices could be further improved by using an ionic-liquid-based gel electrolyte with a wider operation potential and/or combining the pseudocapacitive materials with a 3D graphene framework.[35] With the exceptional mechanical and electrical robustness, the highly interconnected 3D network structure of a graphene hydrogel promises an exciting material for high-performance flexible energy storage devices.

METHODS

1. Graphene Oxide (GO) Synthesis and Purification. GO was prepared by oxidation of natural graphite powder according to the modified Hummers' method.[36,37] Briefly, graphite (3.0 g) was added to concentrated sulfuric acid (70 mL) under stirring at room temperature; then sodium nitrate (1.5 g) was added, and the mixture was cooled to 0 °C. Under vigorous agitation, potassium permanganate (9.0 g) was added slowly to keep the temperature of the suspension lower than 20 °C. Successively, the reaction system was transferred to a 35−40 °C water bath for about 0.5 h, forming a thick paste. Then, 140 mL of water was added, and the solution was stirred for another 15 min. An additional 500 mL of water was added followed by a slow addition of 20 mL of H_2O_2 (30%), turning the color of the solution from brown to yellow. The mixture was filtered and washed with 1:10 HCl aqueous solution (250 mL) to remove metal ions followed by repeated washing with water and centrifugation to remove the acid. The resulting solid was dispersed in water by ultrasonication for 1 h to make a GO aqueous dispersion (0.5 wt %).

2. Preparation of Graphene Hydrogels. The graphene hydrogels can be easily prepared using a modified hydrothermal reduction method.[23,24] Briefly, 0.3 mL of 2 M ascorbic acid aqueous solution was added into 6 mL of 4 mg/mL GO aqueous dispersion, and the mixture was sealed in a Teflon-lined autoclave and maintained at 180 °C for 2 h. The autoclave was naturally cooled to room temperature, and the as-prepared graphene hydrogel was taken out with a tweezer and immersed in 1 M H_2SO_4 aqueous solution overnight for the following experiments.

3. Fabrication of Flexible Solid-State Supercapacitors. First, the H_2SO_4−PVA gel electrolyte was prepared as follows: 1 g of H_2SO_4 was added into 10 mL of deionized water, and then 1 g of PVA power was added. The whole mixture was heated to 85 °C under stirring until the solution became clear. Second, the as-prepared graphene hydrogel was cut into rectangular strips with a dried weight of ~3.5 mg and pressed on the gold-coated polyimide substrate (surface resistance about 2 Ω) under a pressure of ~1 MPa to form a thin film with a thickness of ~120 μm and areal mass of ~2 mg/cm^2. In order to assemble the solid-state device, the prepared H_2SO_4−PVA aqueous solution was slowly poured on two graphene hydrogel films and air-dried at room temperature for 12 h to evaporate excess water. Then the two electrodes were pressed together under a pressure of ~1 MPa for 30 min, which allowed the polymer gel electrolyte on each electrode to combine into one thin separating layer to form an integrated device.

4. Characterizations. Graphene hydrogels before and after pressing were freeze-dried, and their morphologies were characterized by SEM (JEOL 6700). All the electrochemical experiments were carried out using VersaSTAT 4 from Princeton Applied Research. The electrochemical impedance spectroscopy measurements were performed over a frequency range from 10^5 to 10^{-2} Hz at an amplitude of 10 mV. The cycle life tests were conducted by galvanostatic charge/discharge measurements with a constant current density of 10 A/g for 10 000 cycles. The specific capacitance derived from CV curves was calculated according to the following equation: $C = 2(\int I dV)/\nu m\Delta V$, where I is the voltammetric current, m is the graphene mass of one electrode, ν is the potential scan rate, and V is the potential in one sweep segment. The specific capacitance derived from galvanostatic discharge curves was calculated based on the following equation: $C = 2(I\Delta t)/(m\Delta V)$, where I is the discharge current, Δt is the time for a full discharge, m is the graphene mass of one electrode, and ΔV represents the potential change after a full discharge. The energy density (E) and power density (P) of one electrode depicted in the Ragone plots were calculated by using the equations $E = (1/8)C\Delta V^2$ and $P = E/\Delta t$, respectively, where C is the specific capacitance, ΔV is the potential change after a full discharge, and Δt is the time for a full discharge. For the leakage current test, the device was first charged to 1.0 V at 2 mA, and then the potential was kept at 1.0 V for 2 h while acquiring the current data. For the self-discharge test, the device was first charged to 1.0 V at 2 mA and kept at 1.0 V for 15 min, and then the open potential of the device was measured by a digital multimeter as a function of time. For the aqueous electrolyte test, two identical electrodes were separated by a filter paper by clipping and dipped in a 1 M H_2SO_4 solution.

Conflict of Interest: The authors declare no competing financial interest.

Acknowledgment. We acknowledge the Electron Imaging Center for Nanomachines (EICN) at the California NanoSystems Institute for the technical support of TEM. X.D. acknowledges partial financial support by a 3M Nontenured Faculty Award and a Dupont Young Professor Award.

Supporting Information Available: Experimental details and additional figures. This material is available free of charge *via* the Internet at http://pubs.acs.org.

REFERENCES AND NOTES

1. Ju, S.; Facchetti, A.; Xuan, Y.; Liu, J.; Ishikawa, F.; Ye, P.; Zhou, C.; Marks, T. J.; Janes, D. B. Fabrication of Fully Transparent Nanowire Transistors for Transparent and Flexible Electronics. *Nat. Nanotechnol.* **2007**, *2*, 378–384.
2. Cao, Q.; Kim, H.-S.; Pimparkar, N.; Kulkarni, J. P.; Wang, C.; Shim, M.; Roy, K.; Alam, M. A.; Rogers, J. A. Medium-Scale Carbon Nanotube Thin-Film Integrated Circuits on Flexible Plastics Substrates. *Nature* **2008**, *454*, 495–500.
3. Kim, D. H.; Lu, N.; Ma, R.; Kim, Y. S.; Kim, R. H.; Wang, S.; Wu, J.; Won, S. M.; Tao, H.; Islam, A.; *et al*. Epidermal Electronics. *Science* **2011**, *333*, 838–843.
4. Nishide, H.; Oyaizu, K. Toward Flexible Batteries. *Science* **2008**, *319*, 737–738.
5. Simon, P.; Gogotsi, Y. Materials for Electrochemical Capacitors. *Nat. Mater.* **2008**, *7*, 845–854.
6. Hall, P. J.; Mirzaeian, M.; Fletcher, S. I.; Sillars, F. B.; Rennie, A. J. R.; Shitta-Bey, G. O.; Wilson, G.; Cruden, A.; Carter, R. Energy Storage in Electrochemical Capacitors: Designing Functional Materials to Improve Performance. *Energy Environ. Sci.* **2010**, *3*, 1238–1251.
7. Wang, G. P.; Zhang, L.; Zhang, J. J. A Review of Electrode Materials for Electrochemical Supercapacitors. *Chem. Soc. Rev.* **2012**, *41*, 792–828.
8. Meng, C.; Liu, C.; Chen, L.; Hu, C.; Fan, S. Highly Flexible and All-Solid-State Paperlike Polymer Supercapacitors. *Nano Lett.* **2010**, *10*, 4025–4031.
9. Kaempgen, M.; Chan, C. K.; Ma, J.; Cui, Y.; Gruner, G. Printable Thin Film Supercapacitors Using Single-Walled Carbon Nanotubes. *Nano Lett.* **2009**, *9*, 1872–1876.
10. Kang, Y. J.; Chun, S. J.; Lee, S. S.; Kim, B. Y.; Kim, J. H.; Chung, H.; Lee, S. Y.; Kim, W. All-Solid-State Flexible Supercapacitors Fabricated with Bacterial Nanocellulose Papers, Carbon Nanotubes, and Triblock-Copolymer Ion Gels. *ACS Nano* **2012**, *6*, 6400–6406.
11. Kang, Y. J.; Chung, H.; Han, C. H.; Kim, W. All-Solid-State Flexible Supercapacitors Based on Papers Coated with Carbon Nanotubes and Ionic-Liquid-Based Gel Electrolytes. *Nanotechnology* **2012**, *23*, 065401.
12. Hu, S.; Rajamani, R.; Yu, X. Flexible Solid-State Paper Based on Carbon Nanotube Supercapacitor. *Appl. Phys. Lett.* **2012**, *100*, 104103.
13. El-Kady, M. F.; Strong, V.; Dubin, S.; Kaner, R. B. Laser Scribing of High-Performance and Flexible Graphene-Based Electrochemical Capacitors. *Science* **2012**, *335*, 1326–1330.
14. Weng, Z.; Su, Y.; Wang, D.-W.; Li, F.; Du, J.; Cheng, H.-M. Graphene-Cellulose Paper Flexible Supercapacitors. *Adv. Energ. Mater.* **2011**, *1*, 917–922.
15. Choi, B. G.; Hong, J.; Hong, W. H.; Hammond, P. T.; Park, H. Facilitated Ion Transport in All-Solid-State Flexible Supercapacitors. *ACS Nano* **2011**, *5*, 7205–7213.
16. Choi, B. G.; Chang, S. J.; Kang, H. W.; Park, C. P.; Kim, H. J.; Hong, W. H.; Lee, S.; Huh, Y. S. High Performance of a Solid-State Flexible Asymmetric Supercapacitor Based on Graphene Films. *Nanoscale* **2012**, *4*, 4983–4988.
17. Yuan, L.; Lu, X. H.; Xiao, X.; Zhai, T.; Dai, J.; Zhang, F.; Hu, B.; Wang, X.; Gong, L.; Chen, J.; *et al*. Flexible Solid-State Supercapacitors Based on Carbon Nanoparticles/MnO_2 Nanorods Hybrid Structure. *ACS Nano* **2012**, *6*, 656–661.
18. Stoller, M. D.; Park, S.; Zhu, Y.; An, J.; Ruoff, R. S. Graphene-Based Ultrasupercapacitors. *Nano Lett.* **2008**, *8*, 3498–3502.
19. Stoller, M. D.; Ruoff, R. S. Best Practice Methods for Determining an Electrode Material's Performance for Ultracapacitors. *Energy Environ. Sci.* **2010**, *3*, 1294–1301.
20. Huang, Y.; Liang, J. J.; Chen, Y. S. An Overview of the Applications of Graphene-Based Materials in Supercapacitors. *Small* **2012**, *8*, 1805–1834.
21. Xu, Y. X.; Shi, G. Q. Assembly of Chemically Modified Graphene: Methods and Applications. *J. Mater. Chem.* **2011**, *21*, 3311–3323.
22. Li, C.; Shi, G. Q. Three-Dimensional Graphene Architectures. *Nanoscale* **2012**, *4*, 5549–5563.
23. Xu, Y. X.; Sheng, K. X.; Li, C.; Shi, G. Q. Self-Assembled Graphene Hydrogel *via* a One-Step Hydrothermal Process. *ACS Nano* **2010**, *4*, 4324–4330.
24. Sheng, K. X.; Xu, Y. X.; Li, C.; Shi, G. Q. High-Performance Self-Assembled Graphene Hydrogels Prepared by Chemical Reduction of Graphene Oxide. *New Carbon Mater.* **2011**, *26*, 9–15.
25. Zhang, L.; Shi, G. Q. Preparation of Highly Conductive Graphene Hydrogels for Fabricating Supercapacitors with High Rate Capability. *J. Phys. Chem. C* **2011**, *115*, 17206–17212.
26. Chen, J.; Sheng, K. X.; Luo, P. H.; Li, C.; Shi, G. Q. Graphene Hydrogels Deposited in Nickel Foams for High-Rate Electrochemical Capacitors. *Adv. Mater.* **2012**, *24*, 4569–4573.
27. Chen, W. F.; Yan, L. F. *In Situ* Self-Assembly of Mild Chemical Reduction Graphene for Three-Dimensional Architectures. *Nanoscale* **2011**, *3*, 3132–3137.
28. Zhang, X. T.; Sui, Z. Y.; Xu, B.; Yue, S. F.; Luo, Y. J.; Zhan, W. C.; Liu, B. Mechanically Strong and Highly Conductive Graphene Aerogel and Its Use as Electrodes for Electrochemical Power Sources. *J. Mater. Chem.* **2011**, *21*, 6494–6497.
29. Wu, Z. S.; Winter, A.; Chen, L.; Sun, Y.; Turchanin, A.; Feng, X. L.; Mullen, K. Three-Dimensional Nitrogen and Boron Co-Doped Graphene for High-Performance All-Solid-State Supercapacitors. *Adv. Mater.* **2012**, *24*, 5130–5135.
30. Conway, B. E. Electrochemical Supercapacitors: Scientific, *Fundamentals and Technological Applications*; Plenum: New York, 1999; pp 560−561.
31. Jost, K.; Perez, C. R.; McDonough, J. K.; Presser, V.; Heon, M.; Dion, G.; Gogotsi, Y. Carbon Coated Textiles for Flexible Energy Storage. *Energy Environ. Sci.* **2011**, *4*, 5060–5067.
32. Meng, F. H.; Ding, Y. Sub-Micrometer-Thick All-Solid-State Supercapacitors with High Power and Energy Densities. *Adv. Mater.* **2011**, *23*, 4098–4102.
33. Yuan, L. Y.; Yao, B.; Hu, B.; Huo, K. F.; Chen, W.; Zhou, J. Polypyrrole-Coated Paper for Flexible Solid-State Energy Storage. *Energy Environ. Sci.* **2013**, *6*, 470–476.
34. Yang, X. W.; Zhu, J. W.; Qiu, L.; Li, D. Bioinspired Effective Prevention of Restacking in Multilayered Graphene Films: Towards the Next Generation of High-Performance Supercapacitors. *Adv. Mater.* **2011**, *23*, 2833–2838.
35. Xu, Y. X.; Huang, X. Q.; Lin, Z. Y.; Zhong, X.; Huang, Y.; Duan, X. F. One-Step Strategy to Graphene/$Ni(OH)_2$ Composite Hydrogels as Advanced Three-Dimensional Supercapacitor Electrode Materials. *Nano Res.* **2013**, *6*, 65–76.
36. Hummers, W. S.; Offeman, R. E. Preparation of Graphitic Oxide. *J. Am. Chem. Soc.* **1958**, *80*, 1339.
37. Xu, Y. X.; Zhao, L.; Bai, H.; Hong, W. J.; Li, C.; Shi, G. Q. Chemically Converted Graphene Induced Molecular Flattening of 5,10,15,20-Tetrakis(1-methyl-4-pyridinio)porphyrin and Its Application for Optical Detection of Cadmium(II) Ions. *J. Am. Chem. Soc.* **2009**, *131*, 13490–13497.